

Preparation and chemical properties of π -conjugated poly(1,10-phenanthroline-3,8-diyl)s with crown ether subunits



Hiroki Fukumoto, Yumiko Kase, Take-aki Koizumi, Takakazu Yamamoto*

Chemical Resources Laboratory, Tokyo Institute of Technology, 4259 Nagatsuta, Midori-ku, Yokohama 226-8503, Japan

ARTICLE INFO

Article history:

Received 6 February 2014

Received in revised form 9 May 2014

Accepted 12 May 2014

Available online 17 May 2014

Keywords:

π -Conjugated polymers

Poly(1,10-phenanthroline)

Crown ether

Alkaline metal ions

Ru complex

Organometallic polymerization

ABSTRACT

π -Conjugated polymers consisting of 1,10-phenanthroline units and crown ether subunits (**Poly-1**, **Poly-2**, and **Poly-3**) were prepared by dehalogenation polycondensation of the corresponding dibromo monomers using a zero-valent nickel complex as a condensing agent. They were characterized by elemental analysis, ^1H NMR and UV–Vis spectroscopies, and cyclic voltammetry (CV). They were partly soluble in CHCl_3 , and the number average molecular weight of the soluble part of **Poly-2**, which had 15-crown-5 subunits, was estimated to be 5300. The polymers exhibited UV–Vis peaks at approximately $\lambda_{\text{max}} = 360$ nm, which was reasonable. Complexation with $[\text{Ru}(\text{bpy})_2]^{2+}$ and alkaline metal ions made the polymer soluble in organic solvents. The complexation of $[\text{Ru}(\text{bpy})_2]^{2+}$ to the 1,10-phenanthroline unit proceeded quantitatively, and the $[\text{Ru}(\text{bpy})_2]^{2+}$ complexes exhibited CV curves characteristic of $[\text{Ru}(\text{N-N})_3]^{2+}$ complexes.

© 2014 Elsevier Ltd. All rights reserved.

1. Introduction

π -Conjugated polymers have been the focus of numerous studies because of their attractive chemical and physical properties [1–8], and they have been functionalized by introducing reactive subunits.

In particular, crown ether groups have been introduced into π -conjugated polymers [9–26]. Chart 1 shows a schematic drawing of two typical types of π -conjugated polymers with crown ether groups.

These crown-ether-functionalized, π -conjugated polymers exhibit interesting electrical conductivity and optical properties and can be employed as metal sensors.

We report the synthesis and basic chemical properties (e.g., UV–Vis absorption, electrochemical response, and reactivity toward metals) of the new A-type 1,10-phenanthroline polymers, **Poly-1**, **Poly-2**, and **Poly-3**, shown in the lower part of Chart 1. These polymers were prepared by organometallic dehalogenation polycondensation of the corresponding dihalogenated monomers using a zero-valent nickel complex as a condensing agent [27,28].

π -Conjugated polymers consisting of *N*-chelating ligand units (e.g., 2,2'-bipyridine (bpy) and 1,10-phenanthroline (Phen) units) have been the subject of many papers, and various poly(pyridine-2,5-diyl)s and poly(1,10-phenanthroline-3,8-diyl)s have been

synthesized [9,27,29–35]. These polymers exhibit interesting electronic and optical properties and functionalities, such as electrical conductivity and light-emitting properties. However, the synthesis of π -conjugated poly(1,10-phenanthroline-3,8-diyl)s with crown ether subunits has not been performed to our knowledge. [35] In **Poly-1**, **Poly-2**, and **Poly-3**, both the crown ether and Phen units can react with metal species, and elucidating the chemical reactivity of these polymers toward metal species will provide further understanding of π -conjugated polymers with crown ether subunits.

The reactions of low-molecular-weight crown-ether-functionalized 1,10-phenanthrolines (especially with metal species) have been reported by Yam and Zu [36,37], Yu [38] and Neumann [39]. However, the chemical and physical properties of these crown-ether-functionalized π -conjugated poly(1,10-phenanthroline)s have not been studied. Polymeric materials are interesting materials not only because of their chemical and physical functionalities, but also because of their potential for use in films or solids.

2. Experiments

2.1. Materials, general procedures, and measurements

Bis(1,5-cyclooctadiene)nickel $[\text{Ni}(\text{cod})_2]$ was prepared according to literature methods [40,41] or used as purchased. 3,8-Dibromo-1,10-phenanthroline (**Br₂Phen**) and 3,8-dibromo-5,6-dihydroxy-1,10-phenanthroline were prepared according to literature methods [33]. Anhydrous solvents (DMF and ethanol) were

* Corresponding author. Tel.: +81 45 924 5961; fax: +81 45 924 5976.

E-mail address: takakazuyamamoto@kir.biglobe.ne.jp (T. Yamamoto).

purchased from Kanto Chemical Co., Inc. (Tokyo, Japan) and stored under N_2 . The polymerization was performed using standard Schlenk techniques under N_2 or Ar. 1H NMR spectra were collected with JEOL Lambda 300, JEOL JNM-EX400, and Bruker ADVANCE III 400 spectrometers. IR spectra were recorded on a JASCO FT/IR 460 PLUS spectrometer. UV–Vis spectra were measured with Shimadzu UV-2550 and UV-3100PC spectrometers, and photoluminescence (PL) spectra were recorded using a Hitachi F4500 spectrometer. The PL quantum yield (Φ) was calculated using a quinine sulfate standard ($\Phi = 54.6\%$ for ca. 10^{-5} M solution in 0.5 M H_2SO_4). 1H NMR spectra recorded on a Bruker ADVANCE III 400 spectrometer and a part of the UV–Vis spectra were obtained by one of the authors (FH) after he moved to Ibaraki University, Japan. Elemental analyses were performed using LECO CHNS-932 and Yanaco YS-10 SX-Elements microanalyzers. ICP-AES (inductively coupled plasma atomic emission spectrometry) was performed with a Shimadzu ICP-S-8100 apparatus. FAB mass spectra were obtained with a JEOL JMS-700 analyzer. ESI-MS data were obtained by Ms. K. Tsutsui of the Institute for Molecular Science using a Waters Micromass LCT spectrometer and MassLynx Ver. 4.0. CH_3CN solutions of Phen compounds (**Br₂Phen** or the monomer) and $M[PF_6]$ ($M = Li, Na, \text{ or } K$) were used for the ESI-MS analysis. TGA (thermogravimetric analysis) curves were obtained using a Shimadzu thermometric TGA-50 system. CV was performed using a Hokuto-Denko (Tokyo, Japan) HSV-100 electrochemical interface. Gel permeation chromatography (GPC) was performed at TOSOH Analysis and Research Center Co., Ltd. (Yokkaichi, Mie, Japan) using a TOSOH HLC-8220GPC apparatus with 10 mM CF_3COONa in hexafluoro-2-propanol as the eluent and poly(methyl methacrylate) standards.

2.2. Monomer preparation

Monomer-1. NaH (0.17 g, 7.1 mmol) was added to a DMF (50 mL) solution of 3,8-dibromo-5,6-dihydroxy-1,10-phenanthroline (**1**) (1.11 g, 3.0 mmol) at room temperature under N_2 , and the reaction mixture was stirred for 30 min to obtain a dark red mixture. Li_2CO_3 (0.11 g, 1.5 mmol) was added to the reaction mixture. A DMF (ca. 15 mL) solution of triethylene glycol di-*p*-tosylate (1.5 g, 3.3 mmol) was slowly added at room temperature, and the mixture was stirred at 80 °C for 24 h. After cooling to room temperature, the mixture was extracted with chloroform (three times).

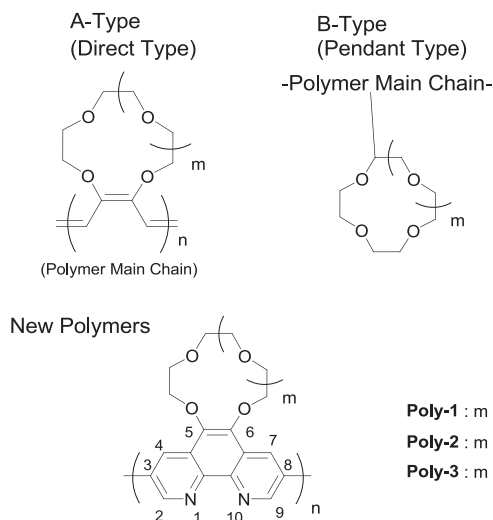


Chart 1. Top: schematic drawing of two typical types of π -conjugated polymers with the crown ether subunits. A-Type: the crown ether group is directly attached to the π -conjugated polymer main chain. B-Type: the π -conjugated polymer has pendant crown ether subunits. Bottom: newly synthesized A-Type π -conjugated polymers with a 1,10-phenanthroline main chain and crown ether subunits.

The combined extracts were washed with water and dried over Na_2SO_4 , and the solvent was removed by evaporation. The crude product was purified by column chromatography on silica (eluent = ethyl acetate) to yield **Monomer-1** (0.93 g, 64%) as a white solid. 1H NMR ($CDCl_3$, 400 MHz) δ 9.11 (d, 2H, $J = 2.2$ Hz, 2,9-H of the Phen unit), 8.68 (d, 2H, $J = 2.2$ Hz, 4,7-H of the Phen unit), 4.48 (m, 4H), 4.05 (m, 4H), 3.89 (s, 4H) ppm. IR (KBr) 1606, 1582, 1442, 1420 cm^{-1} . Anal. Calcd. for $C_{18}H_{16}Br_2N_2O_4$: C, 44.66; H, 3.33; N, 5.79; Br, 33.01%. Found: C, 44.54; H, 3.28; N, 5.69; Br, 32.15%. MS (FAB) $m/z = 485$ ($M + H^+$).

Monomer-2 and **Monomer-3** were prepared using analogous procedures.

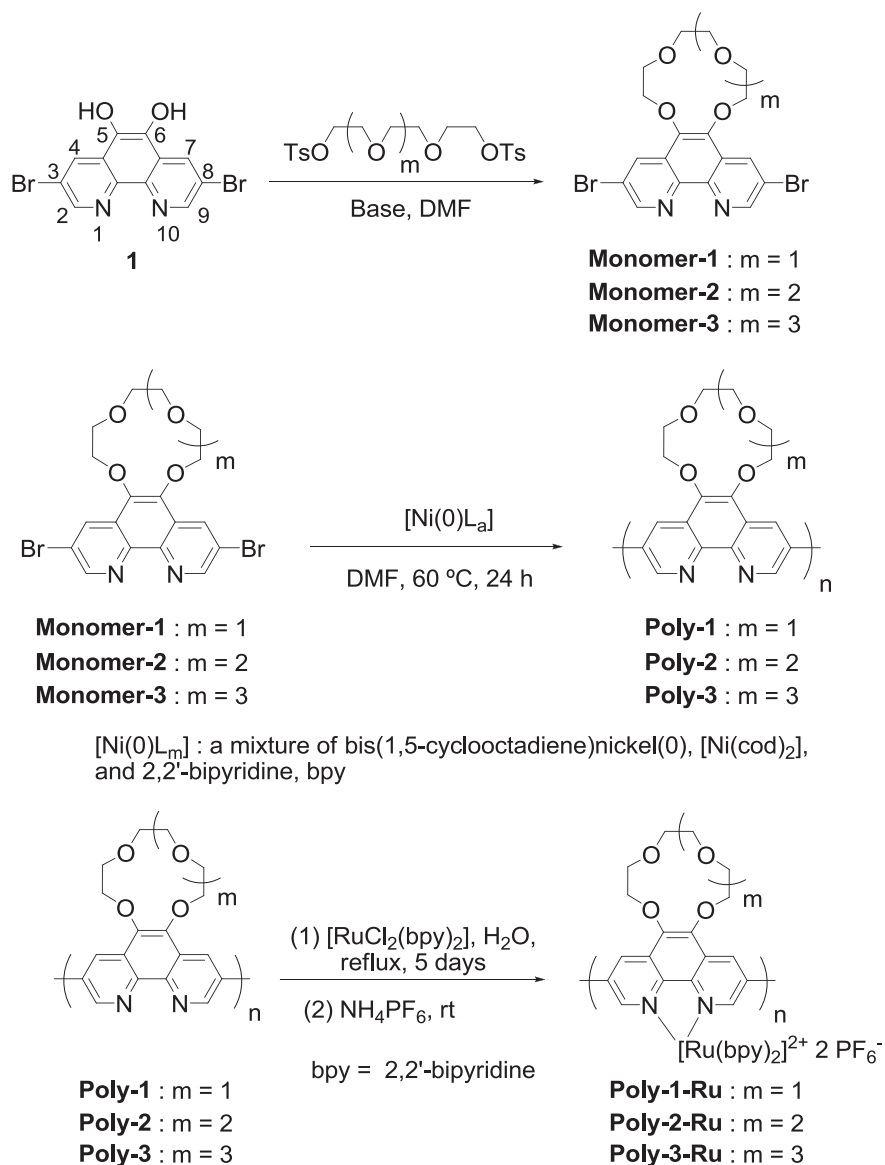
Monomer-2. White solid. 25% yield. 1H NMR ($CDCl_3$, 300 MHz) δ 9.10 (d, 2H, $J = 2.4$ Hz, 2,9-H of the Phen unit), 8.67 (d, 2H, $J = 2.4$ Hz, 4,7-H of the Phen unit), 4.47 (t, 4H, $J = 6.2$ Hz), 4.09 (t, 4H, $J = 6.2$ Hz), 3.82 (m, 4H), 3.79 (m, 4H) ppm. IR (KBr) 1607, 1581, 1437, 1420 cm^{-1} . Anal. Calcd. for $C_{20}H_{20}Br_2N_2O_5$: C, 45.48; H, 3.82; N, 5.30; Br, 30.26%. Found: C, 45.27; H, 3.72; N, 5.30; Br, 30.35%. MS (FAB) $m/z = 529$ ($M + H^+$). The molecular structure of **Monomer-2** was confirmed by X-ray crystallography.

Monomer-3. White solid. 24% yield. 1H NMR ($CDCl_3$, 300 MHz) δ 9.09 (d, 2H, $J = 2.4$ Hz, 2,9-H of the Phen unit), 8.72 (d, 2H, $J = 2.4$ Hz, 4,7-H of the Phen unit), 4.49 (m, 4H), 4.03 (m, 4H), 3.81 (m, 4H), 3.79 (m, 4H), 3.71 (s, 4H) ppm. IR (KBr) 1606, 1582, 1442, 1420 cm^{-1} . Anal. Calcd. for $C_{22}H_{24}Br_2N_2O_6$: C, 46.18; H, 4.23; N, 4.90; Br, 27.93%. Found: C, 45.99; H, 4.26; N, 4.90; Br, 27.50%. MS (FAB) $m/z = 572$ (M^+). The molecular structure of **Monomer-3** was confirmed by X-ray crystallography.

2.3. Polymer preparation

Poly-1. **Monomer-1** (0.48 g, 1.0 mmol) was added to a DMF (50 mL) solution containing $[Ni(cod)_2]$ (0.33 g, 1.2 mmol), 1,5-cyclooctadiene (0.6 mL, 5 mmol), and bpy (0.19 g, 1.2 mmol), and the mixture was stirred at 60 °C for 24 h. After removing approximately half of the solvent by evaporation, the reaction mixture was poured into aqueous ammonia to obtain a dark brown precipitate. The precipitate was separated by filtration, and washed with (i) an aqueous ammonium–methanol solution of dimethylglyoxime and HCl–acidic methanol alternatively (10 times total), (ii) aqueous ammonia–basic methanol (twice), and (iii) a water–methanol mixture (once) in succession. The precipitate was dried under vacuum to obtain **Poly-1** (0.15 g, 46%) as a yellow–brown solid. Some of the polymer seemed to be lost during the work-up, particularly during repeated washing. 1H NMR ($CDCl_3$, 300 MHz) of the $CHCl_3$ -soluble part: δ 9.59 (1.73H, 2,9-H of the inner Phen unit), 9.20 (0.27H, 2,9-H of the terminal Phen unit), 8.94 (1.73H, 4,7-H of the inner Phen unit), 8.61 (0.27H, 4,7-H of the terminal Phen unit), 7.71 (0.27H, 3,8-H of the terminal Phen unit), 4.62–4.55 (4H), 4.14 (4H), 3.94 (4H) ppm. IR (KBr) 1614, 1434 cm^{-1} . Anal. Calcd. for $(C_{18}H_{16}N_2O_4 \cdot 2H_2O)_n$: C, 59.99; H, 5.59; N, 7.77%. Found: C, 59.62; H, 5.28; N, 8.08%. Br was not detected. The polymer appears to be hydrated similarly to 1,10-phenanthroline and reported polypyridines. It was difficult to remove the waters of hydration completely. **Poly-2** and **Poly-3** were prepared following analogous procedures.

Poly-2. Yellow–brown solid. 41% yield. 1H NMR ($CDCl_3$, 300 MHz) of the $CHCl_3$ -soluble part: δ 9.60 (1.86H, 2,9-H of the inner Phen unit), 9.18 (0.14H, 2,9-H of the terminal Phen unit), 8.98 (1.86H, 4,7-H of the inner Phen unit), 8.62 (0.14H, 4,7-H of the terminal Phen unit), 7.70 (0.14H, 3,8-H of the terminal Phen unit), 4.63–4.56 (4H), 4.19 (4H), 3.87–3.83 (8H) ppm. IR (KBr) 1610, 1430 cm^{-1} . Anal. Calcd. for $(C_{20}H_{20}N_2O_5 \cdot 3H_2O)_n$: C, 56.87; H, 6.20; N, 6.63%. Found: C, 57.02; H, 5.66; N, 5.59%. Br was not detected. The discrepancy between the calculated and experimentally determined values might be due to the high thermal stability of the polymer.



Scheme 1. Synthetic routes for monomers and polymers and complexation of the polymers with $[\text{Ru}(\text{bpy})_2]^{2+}$. L = neutral ligand such as cod (1,5-cyclooctadiene) or bpy; a = number of L.

Poly-3. Yellow–brown solid. 38% yield. ^1H NMR (CDCl_3 , 300 MHz) of the CHCl_3 -soluble part: δ 9.61 (1.73H, 2,9-H of the inner Phen unit), 9.18 (0.27H, 2,9-H of the terminal Phen unit),

9.06 (1.73H, 4,7-H of the inner Phen unit), 8.66 (0.27H, 4,7-H of the terminal Phen unit), 7.69 (0.27H, 3,8-H of the terminal Phen unit), 4.64–4.57 (4H), 4.10 (4H), 3.88–3.83 (8H), 3.74 (4H) ppm.

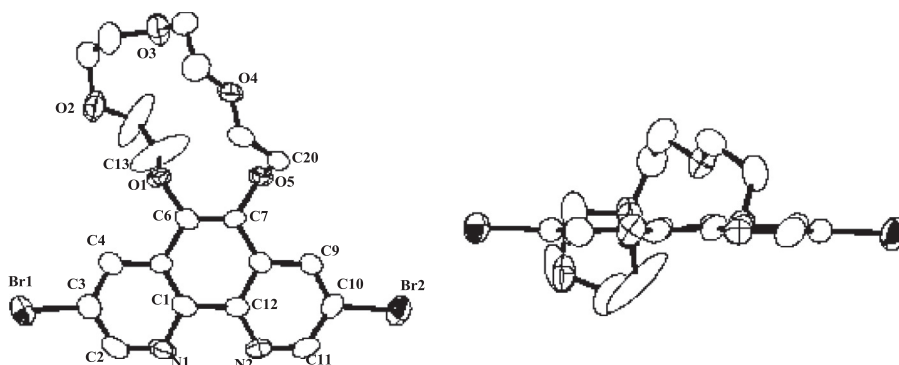


Fig. 1. ORTEP drawing of **Monomer-2** (CCDC No. 921237). Hydrogen atoms are omitted for clarity. Selected bond lengths (Å) and angles ($^\circ$): N1–C1 1.375(11), N1–C2 1.342(15), N2–C11 1.327(14), N2–C12 1.316(13), Br1–C3 1.908(10), Br2–C10 1.892(10), O1–C6 1.402(12), O5–C7 1.392(9), C6–O1–C13 116.0(9), C7–O5–C20 113.9(6).

Table 1
Polymerization results and optical data for **Poly-1–Poly-3**.

Polymer	Yield (%)	M_n^a, M_w^a	λ_{\max} (nm)			λ_{PL} (nm)	
			In CHCl_3	In HCOOH	Film	In CHCl_3 (ϕ^b (%))	Film
Poly-1	46	8900, 47000 (2300)	317 353	325 375	319 363	478 (8.7)	425
Poly-2	41	1400, 15000 (5300)	319 361	330 379	322 377	495 (3.3)	435
Poly-3	38	(2900)	319 357	325 379	319 383	496 (3.7)	424

^a Determined by GPC; for details see the main text. M_n of the CHCl_3 -soluble fraction (ca. 25%), which was determined by ^1H NMR spectroscopy (cf. the main text), is shown in the parentheses.

^b PL quantum yield calculated by comparison to a quinine sulfate standard (ca. 10^{-5} M solution in 0.5 M H_2SO_4 with a quantum yield of 54.6%).

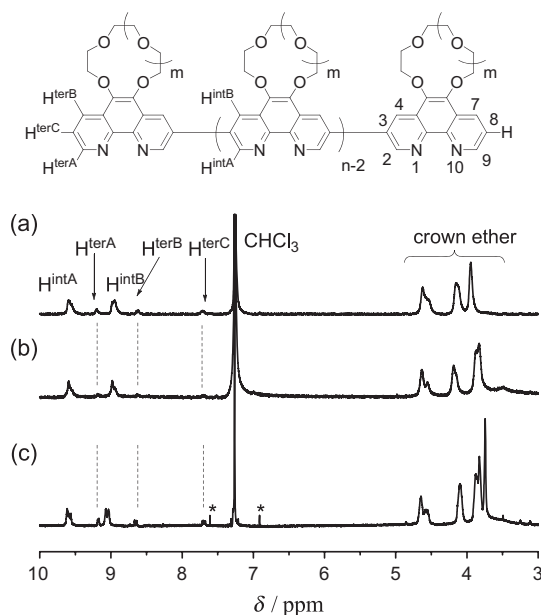


Fig. 2. ^1H NMR spectra of (a) **Poly-1**, (b) **Poly-2**, and (c) **Poly-3** in CDCl_3 . Peaks indicated with a * are spinning side bands.

IR (KBr) 1610, 1431 cm^{-1} . Anal. Calcd. for $(\text{C}_{22}\text{H}_{24}\text{N}_2\text{O}_6 \cdot 2\text{H}_2\text{O})_n$: C, 58.92; H, 6.29; N, 6.25%. Found: C, 58.82; H, 5.75; N, 7.16%. Br was not detected. The discrepancy between the calculated and experimentally determined values might be due to the high thermal stability of the polymer and partial trapping of the ammonium ion by the crown ether unit. The ability of crown ethers to trap the ammonium ion has been reported in the literature [42–44].

2.4. Preparation of Ru(II) complexes of the polymers

A mixture of **Poly-1** (30 mg, 0.10 mmol based on the repeating unit), cis-bis(2,2'-bipyridine)dichloro-ruthenium(II) ($[\text{RuCl}_2(\text{bpy})_2]$; 48.4 mg, 0.10 mmol) and distilled water (10 mL) was stirred under reflux for 5 days under Ar. During the early stages of the reaction, **Poly-1** particles were observed clearly. As the reaction proceeded, the particles disappeared gradually, and a seemingly homogeneous red solution was obtained after 5 days. After cooling the solution to room temperature, the insoluble part was removed by centrifugation. NH_4PF_6 (81.1 mg, 0.50 mmol) was added to the separated soluble part to precipitate a dark red solid. After the solid was separated by filtration, the precipitate was washed with water and dried under reduced pressure to yield **Poly-1-Ru** as a dark red solid (68 mg, 77% yield). ^1H NMR (CD_3CN , 400 MHz) δ 8.8–7.3 (20H, bpy and the Phen unit), 4.5–4.4 (4H), 4.0 (4H), 3.9

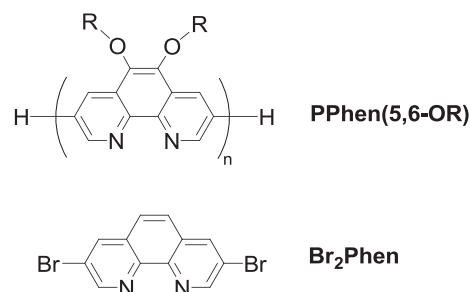


Chart 2. **PPhen(5,6-OR)** prepared by organometallic polycondensation using $[\text{Ni}(\text{O})\text{L}_a]$ and 3,8-dibromo-1,10-phenanthroline (**Br₂Phen**) for the ^1H NMR studies.

(4H) ppm. IR (KBr) 1610, 1445, 842, 556 cm^{-1} . The complexation of **Poly-2** and **Poly-3** to $[\text{RuCl}_2(\text{bpy})_2]$ was performed similarly.

Poly-2-Ru. Yellow–brown solid. Quantitative. ^1H NMR (CD_3CN , 400 MHz) δ 8.8–7.3 (20H, bpy and the Phen unit), 4.5–4.4 (4H), 4.0 (4H), 3.8 (4H), 3.7 (4H) ppm. IR (KBr) 1609, 1445, 842, 556 cm^{-1} .

Poly-3-Ru. Yellow–brown solid. 50% yield. ^1H NMR (CD_3CN , 400 MHz) δ 9.0–7.3 (20H, bpy and Phen unit), 4.6–4.5 (4H), 4.0–3.3 (16H) ppm. IR (KBr): 1609, 1445, 841, 556 cm^{-1} .

2.5. Crystal structure determination

Monomer-2 and **Monomer-3** crystals were obtained for X-ray analysis. For each monomer, a suitable crystal was mounted on a glass fiber. Data collection was performed at -160 °C on a Rigaku/MS Saturn CCD diffractometer with graphite monochromated

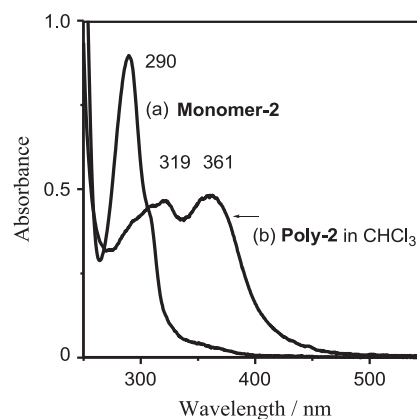


Fig. 3. UV–Vis spectra of (a) **Monomer-2** and (b) **Poly-2** in CHCl_3 .

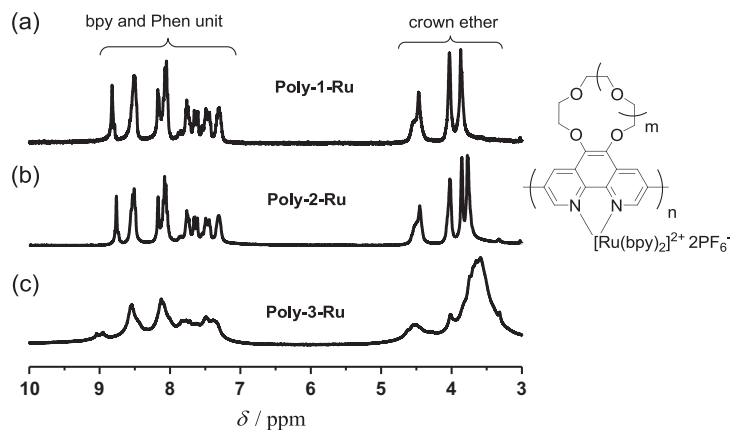


Fig. 4. ^1H NMR spectra of (a) **Poly-1-Ru**, (b) **Poly-2-Ru** and (c) **Poly-3-Ru** in CD_3CN .

$\text{Mo K}\alpha$ radiation ($\lambda = 0.7107 \text{ \AA}$). The data were collected up to a maximum 2θ value of 55° . A total of 720 oscillation images were collected. A data sweep was performed using x scans from -110° to 70° in 0.5° steps, at $\chi = 45.0^\circ$ and $\varphi = 0.0^\circ$. The structures were solved using the Crystal Structure software package [45]. Atomic scattering factors were obtained from the literature. Refinements were performed anisotropically for all non-hydrogen atoms using the full-matrix least-square method. Hydrogen atoms were placed at the calculated positions and were included in the structure calculation without further parameter refinement. The residual electron densities were of no chemical significance. The crystal data and processing parameters are summarized in Table S1 in the Supplementary Material (SM).

3. Results and discussion

3.1. Monomer and polymer preparation

The synthetic routes for the monomers and polymers and their reactions with $[\text{Ru}(\text{bpy})_2]^{2+}$ are shown in Scheme 1.

The diol compound **1** [33] easily reacted with the bis-tosylate compounds ($\text{Ts} = \text{tosyl}$; $m = 1-3$) to yield **Monomer-1**, **Monomer-2**, and **Monomer-3**. The ^1H NMR and IR spectra and elemental analysis data are consistent with their structures (cf. Section 2 and Figs. S1 (^1H NMR) and S2 (IR) in the SM).

The molecular structures of **Monomer-2** and **Monomer-3** were revealed by X-ray crystallography. Fig. 1 shows the molecular

structure of **Monomer-2**, and that of **Monomer-3** is illustrated in Fig. S3a in the SM.

1,10-Phenanthrolines with crown ether subunits that do not contain Br (those with 12-crown-4 [46], 15-crown-5 [38], and 18-crown-6 [47] subunits, which correspond to **Monomer-1**, **Monomer-2**, and **Monomer-3**, respectively) have similar molecular structures with similar bond distances and angles. An analogue of **Monomer-1** without Br (**Phen-12-crown-4**) adopts a packed structure due to $\text{CH}-\pi$ interactions and hydrogen bonds [46]. However, these $\text{CH}-\pi$ interactions and hydrogen bonds are absent in **Monomer-2** and **Monomer-3**. **Phen-12-crown-4** does not exhibit an intermolecular $\pi-\pi$ interaction in the solid state. In contrast, this type of interaction is observed for **Monomer-2** and appears to be assisted by halogen bonding between Br and O as shown in Fig. S3b in the SM.

Poly(1,10-phenanthroline-3,8-diyl)s with crown ether subunits (**Poly-1**, **Poly-2**, and **Poly-3**) were prepared by organometallic polycondensation of **Monomer-1**, **Monomer-2**, and **Monomer-3**, respectively, using a zero-valent nickel complex as a condensing agent [27]. **Poly-1**, **Poly-2**, and **Poly-3** were partially (approximately 1/4) soluble in CHCl_3 and insoluble in organic solvents such as DMF, DMSO and THF. Similarly to poly(pyridine-2,5-diyl)s and previously reported π -conjugated poly(1,10-phenanthroline-3,8-diyl)s [32–34,48], they were more soluble in formic acid. Specifically they were soluble in hot (approximately 60°C) formic acid; however, cooling the solution to room temperature caused the polymer to precipitate. As observed for a poly(pyridine-2,5-diyl) prepared by a similar organometallic polycondensation, **Poly-1**, **Poly-2**, and **Poly-3** did not contain Br, indicating that the polymer–Ni end groups formed during the polymerization were

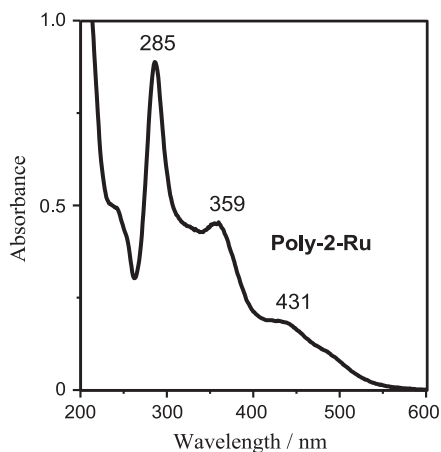


Fig. 5. UV-Vis spectra of **Poly-2-Ru** in CH_3CN .

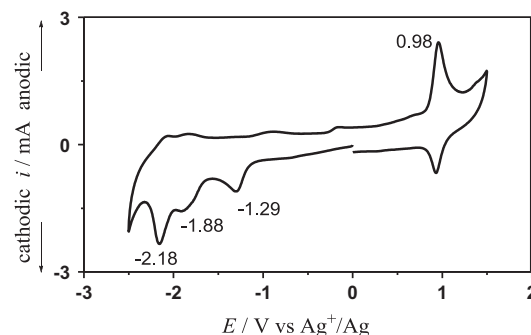


Fig. 6. Cyclic voltammogram of **Poly-1-Ru** in a 0.1 M $[\text{Bu}_4\text{N}]\text{ClO}_4$ solution in CH_3CN . Sweep rate = 50 mV s^{-1} .

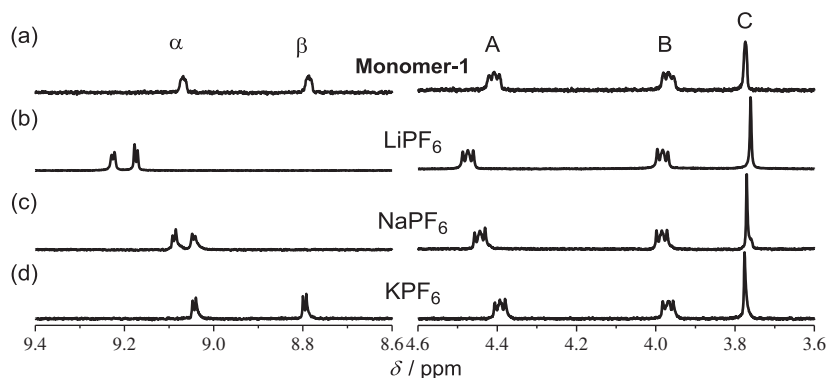


Fig. 7. Changes of ^1H NMR spectra of **Monomer-1** (a) before and (b–d) after the addition of (b) LiPF_6 , (c) NaPF_6 and (d) KPF_6 in CD_3CN . α and β : 2,9-H and 4,7-H of the Phen unit, respectively. A–C: CH_2 groups in the crown ether unit (see Fig. S1b).

transformed into polymer-H end groups during the polymer work-up, which included treating the crude polymer with acid (polymer – $\text{NiL}_a + \text{H}^+ \rightarrow$ polymer-H). The Ni complexes, which might be trapped by the Phen unit, were removed by dimethylglyoxime (see Section 2). The number average molecular weights (M_n s) of the chloroform-soluble polymer parts were estimated from the ^1H NMR data described below. It is assumed that the CHCl_3 -insoluble parts have larger M_n s.

Poly-1 and **Poly-2** were able to be dissolved in hexafluoro-2-propanol (HFIP). When HFIP was used as the eluent in the GPC analysis of **Poly-1**, a unimodal GPC curve was obtained, and **Poly-1** M_n , M_p (peak molecular weight in the GPC curve), and M_w (weight average molecular weight) values were 8900, 21,000, and 47,000 g mol^{-1} , respectively. **Poly-2** exhibited a multimodal GPC curve [49], and the total GPC curve gave M_n and M_w of 1400 and 15,000 g mol^{-1} , respectively. GPC analysis of **Poly-3** was not possible due to its low solubility in HFIP.

Table 1 summarizes the polymerization results and optical properties of **Poly-1**, **Poly-2**, and **Poly-3**.

The IR spectra of the polymers shown in Fig. S4a in the SM are consistent with the polymer structure. The Phen $\nu(\text{C}=\text{N})$ and $\nu(\text{C}=\text{C})$ peaks (or ring vibration peaks) of **Poly-1** are observed at approximately 1600 cm^{-1} . The peak at approximately 1270 cm^{-1} is assigned to the $\nu(\text{C}-\text{O})$ peak of the crown ether subunit.

Fig. 2 shows the ^1H NMR spectra of the **Poly-1–Poly-3** chloroform-soluble parts in CDCl_3 . The ratios of the aliphatic and aromatic peaks areas are consistent with the molecular structures of the polymers.

As shown in Fig. 2, two major aromatic peaks are observed in a 1:1 ratio at approximately δ 9.6 and 9.0 in the ^1H NMR spectra. These peaks are assigned to 2,9-H and 4,7-H of the Phen unit (H^{intA} and H^{intB} in Fig. 2, respectively). Additional peaks appear in the spectra at approximately δ 9.2, 8.6 and 7.7 in a 1:1:1 ratio. The peak at δ 7.7 appears nearly the same position as that of 3,8-H in 1,10-phenanthroline (δ 7.6) [50], and is assigned to the terminal-H of the polymer (H^{terC} in Fig. 2). Thus, the other peaks at δ 9.2 and 8.6 are assigned to 2(or 9)-H and 4(or 7)-H, respectively, of the terminal Phen unit (H^{terA} and H^{terB} , respectively, in Fig. 2). Because the polymers did not contain Br (*vide ante*), the 1:1:1 ratio for the additional peaks is reasonable. Poly(5,6-dialkoxy-1,10-phenanthroline-3,8-diyl) (**PPhen(5,6-OR)**; Chart 2), which was prepared by a similar procedure, also exhibits an H^{terC} peak at δ 7.7 [33].

For **Poly-1**, the intensity ratio of H^{intA} to H^{terA} is approximately 6:1. From these data, the degree of polymerization is calculated to be approximately 7, which corresponds to an M_n of 2300 g mol^{-1} (Table 1). It is assumed that the M_n of the rest chloroform-insoluble part (approximately 3/4 of the polymer) is higher. The M_n s of

Poly-2 and **Poly-3**, which are listed in Table 1, were also estimated from the $\text{H}^{\text{intA}}:\text{H}^{\text{terA}}$ intensity ratios. The M_n of the CDCl_3 -soluble part of **Poly-2** is estimated to be 5300. The ^1H NMR spectra of the polymers in warm formic acid- d_2 could not be collected because the aromatic signals overlapped with the signals of solvent impurities. All the polymers had good thermal stability under N_2 . The TGA results for **Poly-1**, **Poly-2**, and **Poly-3** (Fig. S4b in the SM) show that they undergo a weight loss below 100 $^\circ\text{C}$, which is probably due to the loss of the waters of hydration (see Section 2). The large weight loss observed between 280 and 450 $^\circ\text{C}$ might be due to the decomposition of the crown ether subunit. Increasing the temperature above 450 $^\circ\text{C}$ appears to result in the decomposition of the whole polymer including the Phen unit.

Fig. 3 shows the UV–Vis spectrum of **Poly-2** in CHCl_3 . The $\pi-\pi^*$ transition peak of **Monomer-2** ($\lambda_{\text{max}} = 290$ nm) in CHCl_3 is red-shifted ($\lambda_{\text{max}} = 361$ nm) in **Poly-2** because of the expansion of the π -conjugation system. This λ_{max} value is similar to those of **PPhen(5,6-OR)** (Chart 2) ($\lambda_{\text{max}} = 353\text{--}359$ nm) [33] and is located somewhat higher than that of π -conjugated poly(2-alkyl-1,10-phenanthroline-3,8-diyl) ($\lambda_{\text{max}} = 330$ nm) [51], which might have a twisted main chain due to the steric effects of the 2-alkyl group. In formic acid, **Poly-1**, **Poly-2**, and **Poly-3** exhibit UV–Vis peaks at approximately 380 nm (Table 1), which is similar to the peak position observed for π -conjugated, non-substituted poly(phenanthroline-3,8-diyl) in formic acid [33]. The UV–Vis absorption peaks of **Poly-1**, **Poly-2**, and **Poly-3** in CHCl_3 are slightly red-shifted in cast films (e.g., from 361 nm to 377 nm for **Poly-2**). The small shifts indicate the absence of strong intermolecular electronic interactions between the polymer molecules in the solid state.

Poly-1, **Poly-2**, and **Poly-3** exhibited PL emission peaks in CHCl_3 in the range of 475–500 nm with quantum yields of 3.3–8.7%, which are comparable to that of **PPhen(5,6-OR)** (ca. 4%). UV–Vis and PL data obtained under various conditions are shown in Figs. S5 and S6 and Table S2 in the SM.

3.2. Formation of $[\text{Ru}(\text{bpy})_2]^{2+}$ complexes

Reacting the polymers with $[\text{RuCl}_2(\text{bpy})_2]$ under reflux conditions in water yielded water-soluble polymer complexes (see Scheme 1). The solubility of the products is likely due to their ionic structures. The addition of NH_4PF_6 to the reaction mixtures afforded the water-insoluble precipitates **Poly-1-Ru**, **Poly-2-Ru**, and **Poly-3-Ru**. Similar solubility and precipitation effects due to coordinated $[\text{Ru}(\text{bpy})_2]^{2+}$ and NH_4PF_6 , respectively, were observed for $[\text{Ru}(\text{bpy})_2]^{2+}$ complexes of π -conjugated oligo-(2,2'-bipyridine-5,5'-diyl) and oligo-(2,2'-bipyrimidine-5,5'-diyl) [52]. Low-molecular-weight Phen compounds with crown ether subunits usually react with transition metal complexes (e.g., Re and Ru complexes)

to give products in which transition metals are attached to the Phen unit and not the crown-ether-unit [36–39,47].

As mentioned previously, the polymer-[Ru(bpy)₂]²⁺ complexes were soluble in organic solvents, including CH₃CN, acetone, and DMSO. Fig. 4a shows the ¹H NMR spectrum of **Poly-1-Ru** in CD₃CN. The area ratio of the aromatic to crown ether protons is 1.71:1, which is consistent with the ratio (20:12 or 1.67:1) calculated based on full coordination of [Ru(bpy)₂]²⁺ to the polymer ligand. **Poly-2-Ru** and **Poly-3-Ru** (Fig. 4b and c, respectively) have similar ¹H NMR spectra, which also support the full coordination of [Ru(bpy)₂]²⁺ to the polymer ligands. These data indicate that [Ru(bpy)₂]²⁺ can coordinate to the polymeric compounds quantitatively because of the high affinity of [Ru(bpy)₂]²⁺ for 1,10-phenanthroline.

The ICP-AES results showed that **Poly-2-Ru** contained 9.5% Ru, which is also consistent with the full coordination of [Ru(bpy)₂]²⁺ to the polymer ligand (calculated Ru content = 9.4% for ((C₂₀H₂₀N₂O₅)_n[Ru(bpy)₂]₂PF₆)_n or (C₄₀H₃₆F₁₂N₆O₅P₂Ru)_n). The Ni content was negligible. The IR spectra of **Poly-1-Ru–Poly-3-Ru** and **Poly-1** are shown in Fig. S7 in the SM. In addition to the polymer and bpy aromatic ring and ν(C—O—C) vibrations observed in **Poly-1-Ru–Poly-3-Ru** IR spectra, characteristic PF₆[−] peaks appear at approximately 840 and 560 cm^{−1}.

As shown in Fig. 5, a new peak is observed at 431 nm in the **Poly-2-Ru** UV–Vis spectrum in addition to the π–π* transition peaks of bpy and the original polymer at 285 and 359 nm. This new peak is assigned to MLCT (metal-to-ligand charge transfer). **Poly-1-Ru** and **Poly-3-Ru** exhibit similar UV–Vis spectra, and the UV–Vis spectroscopic data of the polymer complexes are listed in Table S3 in the SM. The intensity of the peak at 431 nm is reasonable for MLCT. The position of the MLCT peak is also typical for [Ru(N–N)₃]²⁺-type complexes, where N–N is an aromatic chelating ligand with two N coordination sites (e.g., [Ru(bpy)₃]²⁺ and a [Ru(bpy)₂]²⁺ complex with oligo-(2,2'-bipyridine-5,5'-diyl)) [52].

Because the polymer complexes are soluble in CH₃CN, their electrochemical responses can be measured with their solutions. Fig. 6 shows the CV curve for **Poly-1-Ru** in a 0.1 M [Bu₄N]ClO₄ (Bu = butyl) solution in CH₃CN. This CV curve is similar to those of [Ru(N–N)₃]²⁺-type complexes such as [Ru(bpy)₃]²⁺ and a [Ru(bpy)₂]²⁺ complex with poly(2,2'-bipyridine-5,5'-diyl) [32,53]. The anodic peak at E_{pa} = 0.98 V vs Ag⁺/Ag is assigned to the oxidation of Ru(II) to Ru(III). In the reduction region, three peaks at E_{pc} = −1.29, −1.88 and −2.18 V vs Ag⁺/Ag are observed, which is typical for [Ru(N–N)₃]²⁺-type complexes. The CV curve of a **Poly-2** film [54] cast on a Pt plate exhibits a reduction peak at about E_{pc} = −2.2 V vs Ag⁺/Ag, which is similar to that of **PPhen(5,6-OR)** (Chart 2).

3.3. Reactivity of the monomers and polymers toward alkaline metal ions

Fig. 7 shows the changes in **Monomer-1** ¹H NMR spectra upon addition of excess MPF₆ (M = Li, Na, K).

The addition of excess LiPF₆ significantly enhances the solubility of **Monomer-1** in CH₃CN. As shown in Fig. 7, the Phen peaks undergo obvious changes upon addition of LiPF₆ and NaPF₆. However, the crown ether signals are only slightly shifted, indicating that Li⁺ and Na⁺ coordinate mainly to the Phen unit (not to the crown ether unit). The addition of LiPF₆ and NaPF₆ to a CD₃CN solution of 3,8-dibromo-1,10-phenanthroline (**Br₂Phen**, Chart 2) also leads to large changes in its aromatic signals as shown in Fig. S8 in the SM, verifying that Li⁺ and Na⁺ coordinate mainly to **Monomer-1** Phen unit. The data shown in Fig. 7 and S8 indicate that **Monomer-1** and **Br₂Phen** do not have a strong affinity for K⁺.

The effects of the amount of added LiPF₆ on the **Monomer-1** ¹H NMR were determined using a 1:6 (vol/vol) CD₃CN:CDCl₃ mixed

solvent, and the results are shown in Fig. S9a in the SM. It is assumed that the sample solution contains both **Monomer-1** and Li⁺-coordinated **Monomer-1** (**Monomer-1-Li**). The NMR data shown in Fig. S9a in the SM indicate rapid chemical exchange between **Monomer-1** and **Monomer-1-Li** on the NMR time scale because only one signal is observed for 2,9-H (at approximately δ 9.0 without LiPF₆) and 4,7-H (at approximately δ 8.6 without LiPF₆). The procedures to prepare the NMR samples for the data collection shown in Fig. S9a are described below the figure. Fig. S9b shows the dependence of the aromatic 4,7-H chemical shift on the amount of added LiPF₆. A comparison of the ¹H NMR data shown in Fig. S1a and part (a) of Fig. S9a shows that the **Monomer-1** aromatic (4,7-H and 2,9-H) signals appear at similar positions in CDCl₃ (Fig. S1a) and in the 6:1 CDCl₃:CD₃CN mixture (Fig. S9a). However, the **Monomer-1-Li** 4,7-H and 2,9-H signal positions appear to be affected by the nature of the solvent, as shown in part (b) of Fig. 7 and part (h) of Fig. S9a.

Under the rapid-exchange conditions, the chemical shifts of the **Monomer-1** and **Monomer-1-Li** peaks are averaged to give one NMR signal. The position of the newly obtained NMR signal reflects the ratio of these two chemical species, and the molar ratio of **Monomer-1** to **Monomer-1-Li** can be calculated from the NMR peak position. Fig. S9b in the SM shows the change in the shift (Δδ) of the chemical shift of the 4,7-H peak as a function of the amount of LiPF₆. As shown in Fig. S9b, Δδ appears to reach a maximum of approximately Δδ = 0.12–0.13 as the amount of LiPF₆ increases. The data shown in Fig. S9b suggest that the **Monomer-1**/**Monomer-1-Li** ratio is 1 when [LiPF₆]/[**Monomer-1**] = 0.7. At this **Monomer-1**/**Monomer-1-Li** ratio, the Li⁺ concentration is estimated to be approximately 0.7 mM, which corresponds to an association constant K = [**Monomer-1-Li**]/[**Monomer-1**][Li⁺] of approximately 1400 M^{−1} (see the caption of Fig. S9b). The **Monomer-1** UV–Vis spectrum does not change significantly upon the addition of LiPF₆.

The **Monomer-1** ESI-MS results obtained in the presence of M[PF₆] (M = Li, Na, K; see Section 2), however, suggest somewhat different complexation mechanism for the monomers and **Br₂Phen** with M⁺, indicating that they behave differently toward MPF₆ under the ESI-MS conditions. The ESI-MS data shown in Table S4 and Fig. S10 in the SM suggest that (1) **Br₂Phen** does not form complexes with alkaline metal cations and (2) **Monomer-1** has a stronger affinity for Na⁺ than Li⁺ under the ESI-MS conditions. **Monomer-2** and **Monomer-3** have a strong affinity for Na⁺ and K⁺ under the ESI-MS conditions as shown in Table S4.

As mentioned previously, **Poly-1**, **Poly-2**, and **Poly-3** exhibited limited solubility in organic solvents. However, the polymers became more soluble in CH₃CN upon the addition of LiPF₆. Fig. S11 in the SM shows the changes in the **Poly-1** ¹H NMR spectrum upon the addition of LiPF₆. Specifically, the Phen-H signals undergo larger shifts than the crown ether-H signals, suggesting that Li⁺ mainly coordinates to the **Poly-1** Phen unit, as is the case for **Monomer-1**.

4. Conclusions

New π-conjugated polymers consisting of the 1,10-phenanthroline (Phen) units and the crown ether subunits (**Poly-1**, **Poly-2**, and **Poly-3**) were prepared, and the molecular structures of the monomers were revealed by X-ray crystallography. A part of the polymer is soluble in CHCl₃, and the M_ns of the soluble parts were estimated to be 2300–5300 based on the ¹H NMR data. The Phen unit has a strong affinity for [Ru(bpy)₂]²⁺, and the complexation of these species makes the polymer soluble. The resulting **Poly-1-Ru–Poly-3-Ru** complexes are electrochemically active and exhibit a reduction peak at approximately −2.1 V vs Ag⁺/Ag. The Phen unit also interacts with M⁺ (M = alkaline metal) [55] and the addition of

LiPF₆ increases the solubility of the polymer. π -Conjugated polymers with crown ether subunits have attracted much interest from the research community, and the present results add new knowledge to the field of π -conjugated polymers and crown ethers.

Acknowledgement

We are grateful to Ms. K. Tsutsui of the Institute for the Molecular Science for the ESI-MS analysis.

Appendix A. Supplementary data

(IR, ¹H NMR, UV–Vis, PL, ESI-MS and CV data and the molecular structure of **Monomer-3**). Supplementary data associated with this article can be found, in the online version, at <http://dx.doi.org/10.1016/j.reactfunctpolym.2014.05.002>.

References

- [1] T.A. Skotheim, J.R. Reynold (Eds.), *Handbook of Conducting Polymers*, third ed., CRC Press, Boca Raton, Florida, 2007.
- [2] H.S. Nalwa (Ed.), *Handbook of Organic Conductive Molecules and Polymers*, John Wiley, Chichester, 1997.
- [3] Y. Chujo (Ed.), *Conjugated Polymer Synthesis*, Wiley-VCH, Weinheim, 2010.
- [4] K. Müllen, J.R. Reynolds, T. Masuda (Eds.), *Conducting Polymers: a Practical Guide to Synthesis*, Royal Soc. Chem, Cambridge, 2014.
- [5] P. Conte, T. Darmanin, F. Guittard, *React. Funct. Polym.* 74 (2014) 40–51.
- [6] H. Wu, B. Qu, D. Tian, Z. Cong, B. Gao, J. Liu, Z. An, C. Gao, L. Xiao, Z. Chen, Q. Gong, W. Wei, *React. Funct. Polym.* 73 (2013) 1432–1438.
- [7] P. Camurlu, N. Karagoren, *React. Funct. Polym.* 73 (2013) 847–853.
- [8] T. Yamamoto, N. Hayashida, *React. Funct. Polym.* 37 (1998) 1–17.
- [9] D.T. McQuade, A.E. Pullen, T.M. Swager, *Chem. Rev.* 100 (2000) 2537–2574.
- [10] M.J. Marsella, T.M. Swager, *J. Am. Chem. Soc.* 115 (1993) 12214–12215.
- [11] D. Demeter, P. Blanchard, I. Grosu, J. Roncali, *J. Incl. Phenom. Macrocycl. Chem.* 61 (2008) 227–239.
- [12] T. Yamamoto, M. Omote, Y. Miyazaki, A. Kashiwazaki, B.-L. Lee, T. Kanbara, K. Osakada, T. Inoue, K. Kubota, *Macromolecules* 30 (1997) 7158–7165.
- [13] Y. Miyazaki, T. Yamamoto, *Chem. Lett.* 23 (1994) 41–44.
- [14] I. Yamaguchi, R. Uehara, *Polym. Int.* 62 (2012) 766–773.
- [15] I. Yamaguchi, H. Mitsuno, *Macromolecules* 43 (2010) 9348–9354.
- [16] H. Cheng, L. Ma, Q.-S. Hu, X.-F. Zheng, J. Anderson, L. Pu, *Tetrahedron Asymmetry* 7 (1996) 3083–3086.
- [17] B. Fabre, J. Simonet, *Coord. Chem. Rev.* 178–180 (1998) 1211–1250.
- [18] S. Scheib, P. Bäuerle, *J. Mater. Chem.* 9 (1999) 2139–2150.
- [19] G. Rimmel, P. Bäuerle, *Synth. Met.* 102 (1999) 1323–1324.
- [20] A. Boldea, I. Lévesque, M. Leclerc, *J. Mater. Chem.* 9 (1999) 2133–2138.
- [21] J. Casanovas, F. Rodríguez-Roperro, D. Zanuy, C. Alemán, *Polymer* 51 (2010) 4267–4272.
- [22] F. Sannicolò, E. Brenna, T. Benincori, G. Zotti, S. Zecchin, G. Schiavon, T. Pilati, *Chem. Mater.* 10 (1998) 2167–2176.
- [23] M. Yu, F. He, Y. Tang, S. Wang, Y. Li, D. Zhu, *Macromol. Rapid Commun.* 28 (2007) 1333–1338.
- [24] H.-H. Lu, Y.-S. Ma, N.-J. Yang, G.-H. Lin, Y.-C. Wu, S.-A. Chen, *J. Am. Chem. Soc.* 133 (2011) 9634–9637.
- [25] S. Karpagam, S. Guhanathan, P. Saktivel, *Polym. Bull.* 68 (2012) 1023–1037.
- [26] J. Zhang, K. Zhang, X. Huang, W. Cai, C. Zhou, S. Liu, F. Huang, Y. Cao, *J. Mater. Chem.* 22 (2012) 12759–12766.
- [27] T. Yamamoto, *Bull. Chem. Soc. Jpn.* 83 (2010) 431–455.
- [28] T. Yamamoto, *Prog. Polym. Sci.* 17 (1992) 1153–1205.
- [29] R.P. Kingsborough, T.M. Swager, *Prog. Inorg. Chem.* 48 (1999) 123–231.
- [30] J.M. Tour, *J. Org. Chem.* 72 (2007) 7477–7496.
- [31] A.S. Abd-El-Aziz, C.E. Carraher Jr., C.U. Pittman Jr., M. Zeldin (Eds.), *Macromolecules Containing Metals and Metal-Like Elements*, vol. 5, Wiley-Interscience, Hoboken, New Jersey, 2005.
- [32] T. Yamamoto, T. Maruyama, Z.-H. Zhou, T. Ito, T. Fukuda, Y. Yoneda, F. Begum, T. Ikeda, S. Sasaki, H. Takezoe, A. Fukuda, K. Kubota, *J. Am. Chem. Soc.* 116 (1994) 4832–4845.
- [33] T. Yamamoto, Y. Saitoh, K. Anzai, H. Fukumoto, T. Yasuda, Y. Fujiwara, B.-K. Choi, K. Kubota, T. Miyamae, *Macromolecules* 36 (2003) 6722–6729.
- [34] Y. Saitoh, T. Yamamoto, *Chem. Lett.* 24 (1995) 785–786.
- [35] Y. Kase, Dissertation for Ms. Degree at Tokyo Institute of Technology, February, 2006.
- [36] M.-J. Li, C.-C. Ko, G.-P. Duan, N. Zhu, V.W.-W. Yam, *Organometallics* 26 (2007) 6091–6098.
- [37] M.-J. Li, Z. Chen, N. Zhu, V.W.-W. Yam, Y. Zu, *Inorg. Chem.* 47 (2008) 1218–1223.
- [38] L.-X. Liu, H.-P. Huang, X. Li, Q.-F. Sun, C.-R. Sun, Y.-Z. Li, S.-Y. Yu, *Dalton Trans.* (2008) 1544–1546.
- [39] J. Etdedgui, Y. Diskin-Posner, L. Weiner, R. Neumann, *J. Am. Chem. Soc.* 133 (2011) 188–190.
- [40] G. Wilke, *Angew. Chem. Int. Ed. Engl.* 27 (1988) 185.
- [41] A. Schunn, S.D. Ittel, M.A. Cushing, R. Baker, R.J. Gilbert, D.P. Madden, *Inorg. Synth.* 28 (1990) 94.
- [42] G. Khayatian, F.S. Karoonian, *J. Chin. Chem. Soc.* 55 (2008) 377–384.
- [43] H.-S. Kim, K.S. Do, K.S. Kim, J.H. Shim, G.S. Cha, H. Nam, *Bull. Korean Chem. Soc.* 25 (2004) 1465–1470.
- [44] H.-C. Sheu, J.-S. Shih, *Anal. Chim. Acta* 324 (1996) 125–134.
- [45] *Crystal Structure, Crystal Analysis Package*, Rigaku and Rigaku/MS, 2000.
- [46] A.S. Denisova, E.M. Dem'yanchuk, G.L. Starova, L.A. Myund, A.A. Makarov, A.A. Simanova, *J. Mol. Struct.* 828 (2007) 1–9.
- [47] C.R. Rice, A. Guerrero, Z.R. Bell, R.L. Paul, G.R. Motson, J.C. Jeffery, M.D. Ward, *New J. Chem.* 25 (2001) 185–187.
- [48] T. Yamamoto, M. Takeuchi, K. Kubota, *J. Polym. Sci., Part B: Polym. Phys.* 38 (2000) 1348–1351.
- [49] The two GPC peak curves showed minor and measure peak curves in approximately 1:3 area ratio peak. The measure GPC peak curve gave M_n , M_p , and M_w of 22,000, 22,000, and 25,000, respectively. The minor GPC peak curve gave M_n , M_p , and M_w of 5600, 5500, and 5700, respectively. An additional small peak curve was observed at a molecular weight of 3000. The total GPC curve was tailed to a low molecular weight region, and this seems to be the reason for the considerably lower M_n compared with M_w . Such tailing sometimes takes place due to technical reasons, and in this case M_p and M_w are more reliable.
- [50] From data base of AIST (National Institute of Advanced Industrial Science and Technology): http://sdbs.db.aist.go.jp/sdbs/cgi-bin/direct_frame_top.cgi.
- [51] T. Yamamoto, K. Anzai, T. Iijima, H. Fukumoto, *Macromolecules* 37 (2004) 3064–3067.
- [52] N. Hayashida, T. Yamamoto, *Bull. Chem. Soc. Jpn.* 72 (1999) 1153–1162.
- [53] N.E. Tokel-Takvoryan, R.E. Hemingway, A.J. Bard, *J. Am. Chem. Soc.* 95 (1973) 6582–6589.
- [54] This film may contain a small amount of formic acid used for the preparation of the film.
- [55] T. Earmme, S.A. Jenekhe, *Adv. Funct. Mater.* 22 (2012) 5126–5136.